Recent Developments in Predicting Unsteady Airloads Caused by Control Surface Motions

W. S. Rowe,* J. D. Sebastian,† and M. C. Redman‡
Boeing Commercial Airplane Company, Renton, Wash.

Solution instabilities are identified within the procedures currently used to predict unsteady aerodynamic loadings on lifting surfaces due to motions of swept hingeline control surfaces. Numerical results are presented that display erratic solution behavior when use is made of various forms of pressure expressions currently employed in control surface analyses. A new expression for the asymptotic pressure function is derived which is formulated to exactly satisfy the change in boundary conditions around the boundary of an oscillating swept hingeline control surface. Results of applying the new pressure function are presented and indicate that stable solutions may be achieved for predicting the unsteady loadings caused by motions of swept hingeline control surfaces.

Nomenclature

b_0	=reference length
c	=local chord length
C_p	=pressure coefficient
i	$=(-1)^{1/2}$
k	=reduced frequency $b_0\omega/V$
$K(x, \xi, y, \eta)$	=kernel function
S	=semispan length
t	=time (sec.)
V	=freestream velocity (length/time)
x, y	=coordinates of downwash station
ξ, η, ζ	=nondimensional coordinates
ξ_c	=hingeline streamwise coordinate
Y_s	=spanwise location of control surface side edge
Θ_H	=hingeline rotation angle in streamwise direction
β	$=(1-M^2)^{1/2}$
$\bar{\beta}$	$=(\beta^2+\tan^2\Lambda)^{1/2}$
Λ	=hingeline sweep angle
ω	=circular frequqncy

Introduction

NUMERICAL methods[1-4] developed to predict unsteady loadings due to control surface motions, using the kernel function approach, have displayed varying degrees of success in maintaining solution accuracy. These methods fail to provide solutions that are relatively invariant with respect to the number of collocation stations used in predicting loadings on a swept hingeline control surface configuration. Some of the problems contributing to the solution instability may now be identified, and new procedures may be incorporated within these methods to assure accurate predictions of unsteady loadings due to control surface motions.

The work of Berman et al.[1] is one of the first attempts made to develop a procedure using the assumed pressure term capable of correctly representing the known singularity functions around the boundaries of control surfaces. However, the resulting solutions have been found to be sensitive to the location and number of collocation stations used in the analysis. The sensitivity may be attributed to the particular solution process being used, which applies the assumption that continuous and discontinuous downwash distributions may be combined to satisfy the discontinuous kinematic boundary conditions at a pre-selected distribution of collocation stations. Changing the control point locations by relatively small amounts results in large changes in the predicted loadings; consequently, this method requires calculation of downwashes at many stations and seeking solutions in the least-square-error sense.

Rather than attempting to combine continuous and discontinuous downwash sheets to satisfy a discontinuous distribution, Landahl[5] suggested that a downwash sheet be first constructed so that it contains identical discontinuities as given by the kinematic distribution. This derived downwash sheet would then be subtracted from the kinematic distribution, resulting in a residual downwash distribution that would be smooth and continuous and for which solutions could be readily obtained by standard lifting surface procedures. Computer programs developed around this procedure using Landahl's prescribed pressure distributions appear to provide converged predictions of unsteady loadings for those particular configurations having zero sweep hingeline control surfaces. However, use of other pressure expressions suggested by Hewitt[4] and Ashley[6] for the swept hingeline case has resulted in solutions that may be highly unstable and very sensitive to the number and distribution of collocation stations used in the analysis.

The present work represents an extension of the analytical procedures suggested by Landahl[5] to provide a capability of accurately predicting unsteady loadings due to motions of swept hingeline control surfaces.

Problem Identification

Numerical studies have been conducted to evaluate the accuracy of predicting the hinge moments on a wing-aileron-tab configuration shown in Fig. 1. The configuration represents the planform of a Boeing 727 for which a vast amount of flight test data are available to make real flow comparison of hinge moments due to tab or aileron rotations. The configuration also includes a relatively large hingeline sweep with controls having a small spanwise length in comparison with the semispan, and should provide a good general analysis configuration that could point out any weakness of the theory in predicting the hinge moments.

Initial theoretical investigation was performed using a standard Gaussian distribution for the distribution of collocation stations. Hinge moments obtained for both the aileron and tab due to individual rotations were compared with flight test data and, surprisingly enough, the theoretical predictions

Presented as Paper 75-101 at the AIAA 13th Aerospace Sciences Meeting, Pasadena, Calif., Jan 20-22, 1975; submitted Feb 18, 1975; revision received March 4, 1976. This research was supported in part by NASA contract NAS1-12020 and the Boeing IR&D program.

Index categories: Aircraft Aerodynamics (including Component Aerodynamics); Nonsteady Aerodynamics.

*Principal Engineer, Flutter Research Unit.

†Applied Mathmatician, Boeing Computer Services, Inc.

‡Engineer, Boeing Computer Services, Inc.

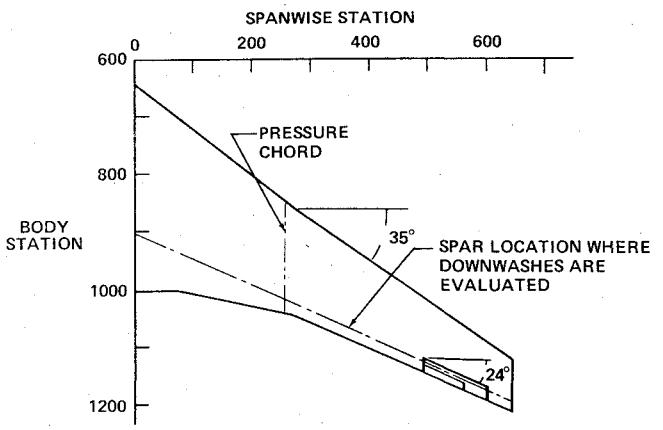

Fig. 1 Analysis planform (727) used to check accuracy of unsteady loading predictons.

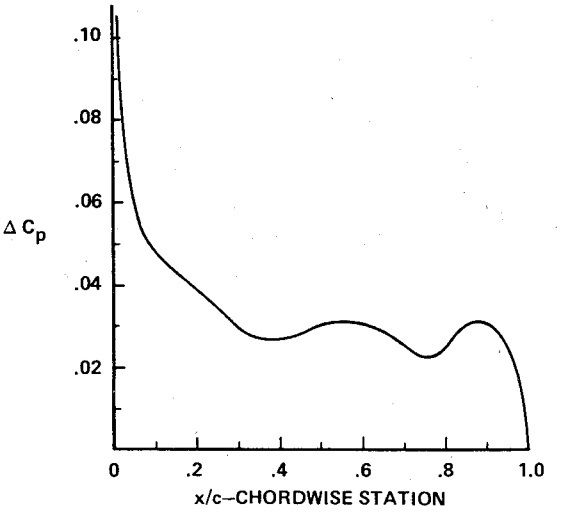

Fig. 2 Chordwise pressure distribution obtained at span station located in Fig. 1.

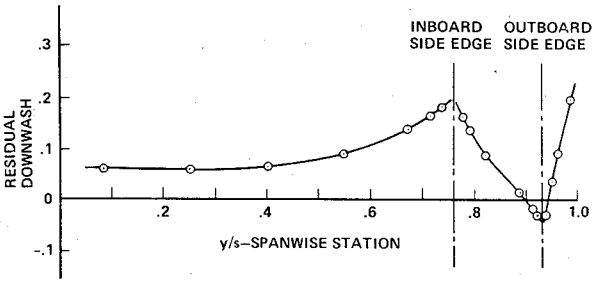

Fig. 3 Residual downwash distribution along wing spar shown in Fig. 1.

were found to be within 6% of the measured hinge moments. The analysis included the use of local linearization of velocity due to thickness effects as described in Ref. 2.

Additional solutions were obtained using a different number of collocation stations within the solution process. Comparison of the theoretical results with experimental data indicated the predicted hinge moments to be in error by approximately 20% of the experimental values. Further numerical investigations verified that the predicted hinge moments depended upon the manner in which the collocation stations were distributed over the surface. It is apparent that the original collocation distribution giving the least error in hinge moment was a rather fortuitous selection. Examining the pressure distributions on the main lifting surface at stations a large distance away from the control surface disclosed the chordwise pressure distributions to be oscillatory and not exhibiting proper characteristics. Figure 2 displays the theoretical chordwise pressure distribution existing on the wing at semispan stations of $y/s=0.4$, which is well away from the control surface side edge located at $y/s=0.76$. It is expected that the chordwise distribution would be monotonically decreasing from leading to trailing edges. However, instead of monotonically decreasing, the distribution is highly wavy, indicating that portions of the highly oscillatory assumed pressure distributions used in the solution process have a large effect on the final solution. Additional numerical experimentations were made to determine the effect of the ratio of spanwise length of the control surface to the semispan length on the solution sensitivity. The analyses were conducted on a 45° sweep constant chord configuration to evaluate the control surface hinge moments for control surface configurations ranging from full-span control surfaces to control surfaces having a very small ratio of control surface length to semispan lengths. The hinge moments obtained for the full-span cases were almost invariant with the distribution of collocation stations. However, some variation was perceived for control surfaces of half-span lengths, and the solutions became progressively unstable as the control surface lengths were reduced to very small ratios of the semispan length.

A plot of the residual downwashes was made to determine how well the incremental downwashes were being calculated. "Residual" downwash is the downwash that remains after the kinematic downwash is subtracted from the downwashed obtained using the pressure developed by the asymptotic expansion process. Figure 3 represents the spanwise variation of the residual downwash plotted for a wing spar that is located just aft of the hingeline defined in Fig. 1.

The residual downwashes should be smooth and continuous since only the kinematic discontinuities were to be removed; and the remaining downwash distribution should not exhibit any other singularity characteristics. However, the spanwise residual distribution of Fig. 3 displays cusps in the distribution at the side edges of the control surface and is contrary to the solution definition of the original boundary value problem.

Other authors have also displayed residual downwashes having cusps at the control surface side edges. Of note is the work of Medan[3] where results of a steady-state analysis is presented for a highly swept planform having a deflected half-span flap. Also, large gradients in residual downwash are shown to exist at the side edges of a half-span control surface configuration on a 45° swept constant chord planform presented by Hewitt.[4] It is evident that severe convergence problems will result for solutions possessing the extreme residual downwash gradients shown in there references.

The solution process suggested by Landahl[5] requires that the residual downwash distribution be smooth and continuous over the entire lifting surface so that it can be approximated by standard lifting surface solution techniques as described in the following.

Solution Process for Discontinuous Downwash Distributions

The solution process developed for lifting surfaces having discontinuous downwash distributions may be described in the matrix equation

$$\{W(x,y)\} - \left\{\int\int \Delta P(\xi,\eta)_{ae} K(\xi,\eta)\, d\xi\, d\eta\right\} = \left[\int\int \Delta P_i(\xi,\eta) K(\xi,\eta)\, d\xi\, d\eta\right] \cdot \{a_i\} \qquad (1)$$

where $\{W(x,y)\}$ is the kinematic downwash obtained from the motion of the lifting surface and containing discontinuities along the edges of a control surface,

$$\int\int \Delta P(\xi,\eta)_{ae} K(\xi,\eta)\, d\xi\, d\eta$$

is the surface downwash distribution that is formulated having identical discontinuities along the control surface edges as defined for the kinematic distribution, $\Delta P(\xi, \eta)_{ae}$ is the pressure distribution developed by the asymptotic expansion process that provides the same change in boundary conditions across the control surface edges as defined within the kinematic distribution, and

$$\int\int \Delta P_i(\xi, \eta) K(\xi, \eta)\, d\xi\, d\eta$$

is the standard lifting surface downwash distribution that is smooth and continuous and is calculated using smooth and continuous assumed pressure distributions $\Delta P_i(\xi,\eta)$ having unknown coefficient multipliers a_i.

The solution process is a two-step process. The first step is to calculate the residual downwash distribution by performing the operation

$$\left\{W(x,y)_{\text{(kinematic)}}\right\} - \left\{\int\int \Delta P(\xi, \eta)_{ae} K(\xi, \eta)\, d\xi\, d\eta\right\} - \left\{W(x,y)_{\text{(residual)}}\right\} \quad (2)$$

The residual distribution is to be smooth and continuous and is used as the boundary condition for the second step, which is the solution of

$$\left\{W(x,y)_{\text{(residual)}}\right\} = \left[\int\int \Delta P_i(\xi,\eta) K(\xi,\eta)\, d\xi\, d\eta\right] \cdot \{a_i\} \quad (3)$$

The final pressure distribution is then the sum of the pressure components, i.e.,

$$\Delta P(\xi,\eta)_{\text{(final)}} = \Delta P(\xi,\eta)_{ae} + \sum_i \Delta P_i(\xi,\eta) \cdot a_i \quad (4)$$

The residual downwashes are required to be smooth and continuous, not only to satisfy the solution technique, but also because the asymptotic expressions originally developed were required to exactly satisfy the basic flow equation and *change* in boundary conditions across the edges of the control surface. Consequently, the subtraction of the *change* in boundary conditions from the kinematic distribution must provide a residual distribution that is smooth and continuous, otherwise, it must be presumed that the asymptotic pressure expressions are insufficient to fully satisfy the original boundary value problem.

Further numerical experimentations were conducted to determine the applicable range of the control surface configuration parameters for which the published pressure expressions may be used.

Numerical Investigation

Initial studies to determine the solution accuracy were conducted on a zero sweep constant chord planform having a 30% chord control surface of various spanwise lengths. The pressure expression used in the analysis is the expression developed by Landahl[5] for the zero sweep rectangular control surface, and for $k=0$ is given as

$$C_p = -\frac{\Theta_H}{\pi\beta} \log\left[\sqrt{(\xi-\xi_c)^2+\beta^2(\eta-y_s)^2} - \beta(\eta-y_s)\right] \quad (5)$$

Analysis results obtained for several spanwise length control surfaces indicate that the residual downwashes were smooth and continuous and that the solution results were almost invariant with the number of collocation stations used in the analysis. Also, the chordwise pressure distributions at stations located at large distances from the control surface side edges were monotonically decreasing in value from the leading edge to trailing edge, and no chordwise waviness was apparent in any of the solutions, including solutions for very small span length control surface.

Solution sensitivities were then obtained using another loading function as suggested by Ashley[6] and as applied in computer program developed by Darras and Dat[7] and by Zwaan.[8] The form of the $k=0$ asymptotic pressure expression of Ref. 6 is given as

$$C_p = -\frac{\Theta_H}{\pi\bar{\beta}} \log\left[\sqrt{(\xi-\xi_c)^2+\beta^2(\eta-y_s)^2} - \beta(\eta-y_s)\right] \quad (6)$$

where

$$\bar{\beta} = \sqrt{\beta^2+\tan^2\Lambda}$$

It should be noted that the only difference between this expression for swept hingelines and Landahl's expression for nonswept hingelines is the factor $\bar{\beta}$ as contained in the multiplying coefficient. Unsteady lifting surface pressure distributions were obtained using the constant chord 25° sweep planform of Ref. 9 shown in Fig. 4 for which experimental lifting surface data are available. Motion of the configuration is composed of an oscillating outboard flap with all other components maintained in a stationary position.

Figure 5 represents the chordwise variation of the in-phase pressure component (ΔC_p real) for a spanwise station located at a large distance from the control surface side edge. Experimental values are represented by the open symbols and two theoretical curves are given which represent the solution results using two distinctly different distributions of collocation stations. The theoretical results for the [4, 6] solution represent the results obtained using four collocation stations on six spanwise downwash chords. The downwash chords are located at relatively large distance from the control surface side edge. Theoretical prediction using the [4, 6] distribution follows the trends of the experimental values, except in the region where the hingeline gap affects the experimental results. The solution results of [7, 9] distribution contain a chordwise waviness near the trailing edge which is thought to be due to having the downwash chords located very near the control surface side edge. The presence of small pressure wave lengths indicates that the residual downwash distribution may not be smooth and continuous across the control surface side edge. As a result, some of the small wave length assumed pressure modes are required to satisfy irregular boundary conditions being generated by the asymptotic pressure function of Eq. (6).

Residual downwashes using the pressure expression of Eq. (6) were obtained for the 45° sweep constant chord planform shown in Fig. 6. Effects of the large hingeline sweep angle on residual downwashes should be well identified in using this configuration since tan Λ becomes equal to the same order of

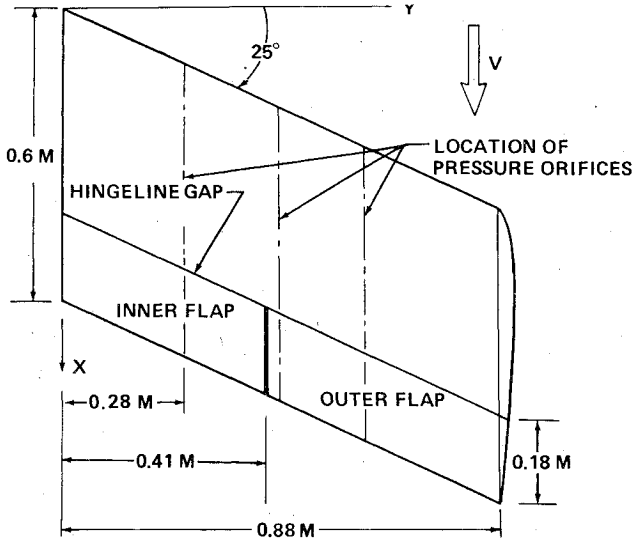

Fig. 4 Experimental planform of Ref. 9 showing the side-by-side control surface arrangement.

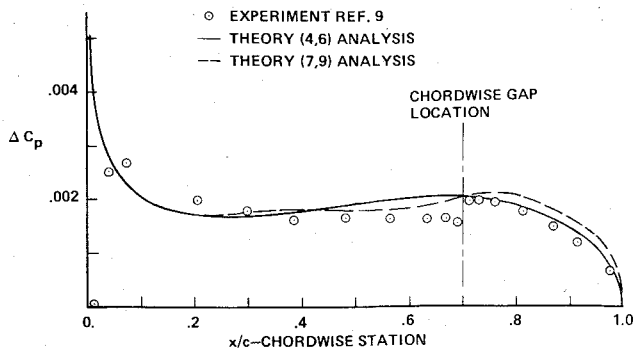

Fig.5 Comparison of theoretical and experimental chordwise variation of in-phase pressure and distribution, $Y=0.28M$.

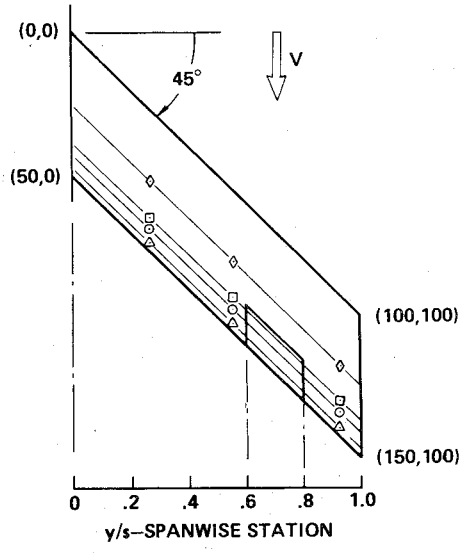

Fig. 6 Analysis planform used to evaluate residual downwash characteristics.

magnitude as β^2. The spanwise variations of the residual downwash for $k=0$ and $M=0$ are shown in Fig. 7. The spanwise variation of residual downwash for stations ahead of the hingeline is smooth and continuous. However, for stations aft of the hingeline, there is a finite discontinuity as well as a slope discontinuity at the side edges of the control surface. This side edge discontinuity may be analytically predicted since it can be shown that the pressure expression will satisfy the boundary condition discontinuity across the hingeline, but will not satisfy the side edge discontinuity condition. Consequently, use of the pressure expression of Eq. (6) should be limited to configurations having zero sweep control surface hingeline, or to configurations having small hingeline sweep angles and large span length control surfaces, with the restriction that the collocation stations are spaced well away from the control surface side edges.

Residual downwashes have also been obtained using the configuration of Fig. 6 and applying another pressure expression that has been used in computer programs developed by Rowe,[2] Medan,[3] and Hewitt.[4] The pressure expression contained in these references for $k=0$ is

$$C_p=-\frac{\Theta_H}{\pi\bar{\beta}}\log\left[\sqrt{(\xi-\xi_c)^2+\bar{\beta}^2(\eta-y_s)}-\bar{\beta}(\eta-y_s)\right] \quad (7)$$

This expression differs from Eq. (6) having $\bar{\beta}$ included within the logarithmic function as well as appearing in the multiplying coefficient.

The residual downwashes shown in Fig. 8 indicate that for chordwise stations ahead of the hingeline, the residual

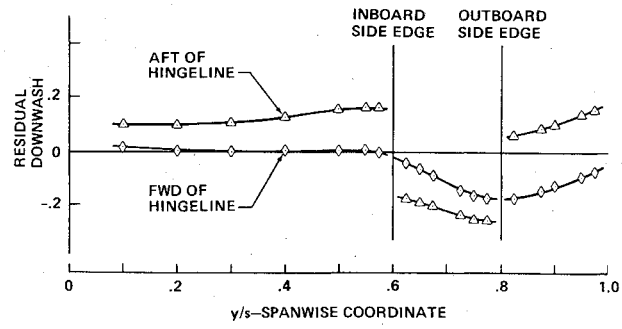

Fig. 7 Spanwise residual downwash distributions along spars forward and aft of hingeline using pressure expressions of Eq. (6).

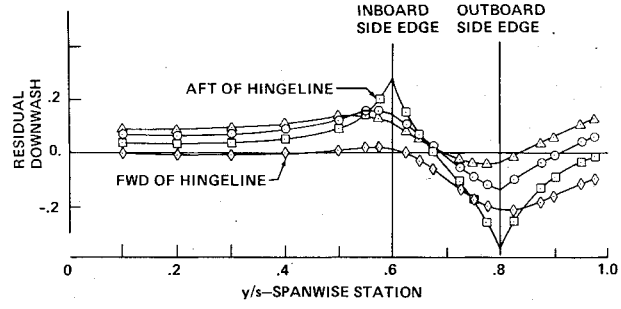

Fig. 8 Spanwise residual downwash distributions along spars foward and aft of hingeline using pressure expression of Eq. (7).

distributions are smooth and continuous across the side edge. However, the distributions have a slope discontinuity across the side edge for stations aft of the hingeline. It was also noted that for small control surface span lengths, the magnitude of the distributions remained the same and the discontinuity peaks were spaced closer together producing a highly localized oscillatory distribution in the residual downwashes. This localized oscillatory distribution in residual downwashes is identified as being the major contribution factor in producing erratic results for small span length control surface analyses.

In order to alleviate the solution sensitivities caused by irregular residual downwashes, new pressure expresssions were obtained by reformulating the asymptotic expansion process following the procedures suggested by Landahl.[5] The step-by-step procedure is presented in the appendix. The $k=0$ pressure expression obtained from the new formulation is given as

$$C_p=-\frac{\Theta_H}{\pi\bar{\beta}}\log\Big[\sqrt{(\xi-\xi_{cs})^2+\beta^2(\eta-y_s)^2}-[\beta^2(\eta-y_s)+(\xi-\xi_{cs})\tan\Lambda]/\bar{\beta}\Big] \quad (8)$$

and the resulting downwash distributions are shown in Figs. 9 for the analysis configuration of Fig. 6. It should be noted that the residual distributions are now smooth and continous for all stations either ahead of, or behind, the hingeline. Further analyses using the new pressure expression of Eq. (8) and applied to the 727 planform of Fig. 1 resulted in predicting hinge moments much closer to the experimental values than had been previously obtained. Also, the chordwise pressure distributions at large spanwise distances away from the control surface were found to be monotonically decreasing in value from the leading edge to the trailing edge. Furthermore, the final lifting surface pressure distributions remain almost invariant with the distribution and number of collocation stations used in the analyses.

Conclusion

The importance was established for the need to calculate smooth residual downwash distributions in order to obtain

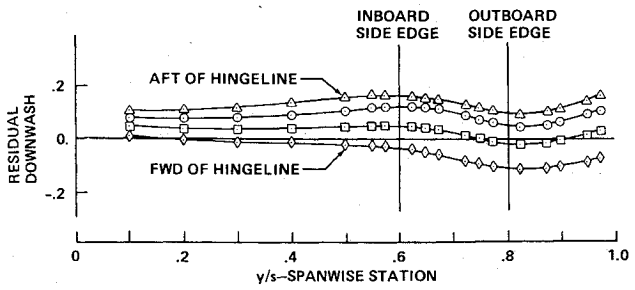

Fig. 9 Spanwise variation of residual downwash distribution using pressure expression of Eq. (8).

stable solutions relatively independent of the number o. collocation stations used in the solution process. It was shown that the use of various forms of pressure expressions currently employed in control surface analyses were inadequate to achieve this result. Therefore, an asymptotic pressure expression was developed following the procedures of Landahl. New pressure expressions were derived that appear to exactly satisfy the boundary conditions for swept and nonswept control surface hingelines. Use of the new pressure expressions results in residual downwashes that are smooth and continuous without exhibiting any discontinuities at the control surface side edges. This should result in predictions of lifting surface pressures that will be almost invariant with the number of collocation stations used in the solution process.

Appendix

Formulation of Pressure Expressions That Satisfy Boundary Conditions on a Swept Hingeline Control Surface

The procedure used to obtain the pressure expressions that satisfy the boundary conditions of a swept hingeline trailing edge control surface is the asymptotic expansion process suggested by Landahl.[5]

The analysis coordinate system is shown in Fig 10 where the coordinates are referenced to the inboard side edge corner.

The linearized boundary value problem is developed in terms of the pressure perturbation $C_p=\bar{P}e^{ikt}$, where the pressure magnitude satisfies the flow equation for sinusoidal motion given as

$$\beta^2\bar{P}_{xx}+\bar{P}_{yy}+\bar{P}_{zz}-2ikM^2\bar{P}_x+k^2M^2\bar{P}=0 \qquad \text{(A1)}$$

having the boundary conditions on the surface of

$$\bar{P}_z=\begin{cases}-2\Theta_H[\delta(x-x_c)+2ik-k^2(x-x_c)]U(y) & \text{for } x\geq x_c\\ 0 & \text{for } x>0\end{cases}$$

$$U(y)=\begin{cases}0 & y<0\\ 1 & y>0\end{cases} \qquad \text{(A2)}$$

The steps involved in obtaining solution of the above boundary value problem are to first scale the x coordinate to simplify Eq. (A1) by letting

$$x_o=x/\beta;\ y_o=y;\ z_o=z$$

Then define

$$x-x_c=x-y\tan\Lambda$$

$$=\beta\left(x_o-y_o\frac{\tan\Lambda}{\beta}\right)$$

$$=\beta(x_o-y_o\tan\Lambda_1)$$

and note that

$$\delta(ax)=\frac{1}{a}\delta(x)$$

Then introduce a new variable, ψ, to remove the first derivative term of Eq. (A1) defined as

$$\bar{P}=e^{ikM^2x_o/\beta}\psi$$

Following this procedure results in the following transformed boundary value problem.

$$\psi_{x_ox_o}+\psi_{y_oy_o}+\psi_{z_oz_o}+\frac{k^2M^2}{\beta^2}\psi=0 \qquad \text{(A3)}$$

$$\frac{\partial\psi}{\partial z_o}=-2\Theta_H\left[\frac{1}{\beta}(x_o-y_o\tan\Lambda_1)+2ik-k^2\beta^2(x_o-y_o\tan\Lambda_1)\right]\cdot e^{-ikM^2x_o/\beta^2}\quad\text{for } x_o\geq y_o\tan\Lambda_1 \qquad \text{(A4)}$$

$$\partial\psi/\partial z_o=0 \quad \text{for } x_o<y_o\tan\Lambda_1$$

To study the lifting surface problem in the vicinity of the control surface corner, all coordinates are scaled by ϵ; that is, let

$$\bar{x}=\frac{x_o}{\epsilon};\ \bar{y}=\frac{y_o}{\epsilon};\ \bar{z}=\frac{z_o}{\epsilon}$$

and expand ψ into a series in powers of ϵ; i.e., $\psi=\psi_0+\epsilon\psi_1+\gamma^2\psi_2+\ldots$ Introducing this new transformation into the boundary value problem of Eqs. (A3) and (A4) and expanding the exponential function in the boundary condition, then collecting terms of like power in ϵ results in the following simplified boundary value problems that are to be solved and summed to satisfy the original boundary value problem.

$$\begin{cases}\Delta^2\psi_o=0 & \text{(zeroth order)}\\ \dfrac{\partial\psi_o}{\partial z_o}=\begin{cases}-2\Theta_H\left[\dfrac{1}{\beta}\delta(\bar{x}-\bar{y}\tan\Lambda_1)\right] & \bar{y}\geq 0\\ 0 & \bar{y}<0\end{cases}\end{cases} \qquad \text{(A5)}$$

$$\begin{cases}\Delta^2\psi_1=0 & \text{(first order)}\\ \dfrac{\partial\psi_1}{\partial z_o}=\begin{cases}-2\Theta_H\left[2ik-\dfrac{ikM^2\bar{x}}{\beta^2}\delta(\bar{x}-\bar{y}\tan\Lambda_1)\right] & \bar{y}\geq 0\\ 0 & \bar{y}<0\end{cases}\end{cases} \qquad \text{(A6)}$$

$$\begin{cases}\Delta^2\psi_2=-\dfrac{k^2M^2}{\beta^2}\psi_o & \text{(second order)}\\ \dfrac{\partial\phi_2}{\partial z_o}=\begin{cases}-2\Theta_H\left[\dfrac{2k^2M^2\bar{x}}{\beta}-k^2\beta(\bar{x}-\bar{y}\tan\Lambda_1)\right.\\ \left.-\dfrac{k^2M^4\bar{x}^2}{2\beta^3}\delta(\bar{x}-\bar{y}\tan\Lambda_1)\right] & \bar{y}\geq 0\\ 0 & \bar{y}<0\end{cases}\end{cases} \qquad \text{(A7)}$$

Since the boundary value problems contain (or can be made to contain) the Laplacian $\nabla^2\psi=0$, use of Green's theorem may be readily applied to obtain solutions of the form

$$\psi(x,y,z)=-\frac{1}{2\pi}\int_{-\infty}^{\infty}\int_{-\infty}^{\infty}\frac{\partial\psi(\bar{x},\bar{y},0)}{\partial\bar{z}}\Big|_{z=0}\frac{d\bar{x}\,d\bar{y}}{(x-\bar{x})^2+(y-\bar{y})^2+z^2)^{1/2}} \qquad \text{(A8)}$$

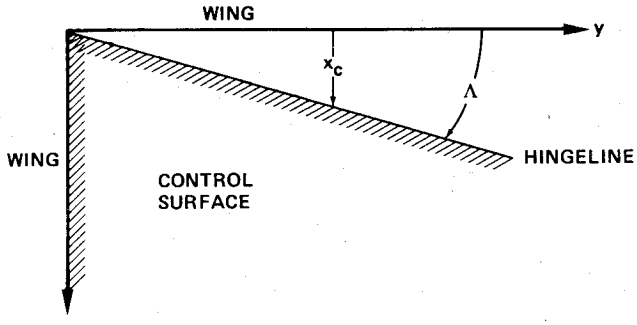

Fig. 10 Analysis coordinate system.

where

$$\left.\frac{\partial \psi(\bar{x}, \bar{y}, 0)}{\partial \bar{z}}\right|_{z=0}$$

represents the surface boundary conditons.

The Green's function developed from method of images is

$$v = \frac{2}{[(x-\bar{x})^2 + (y-\bar{y})^2 + z^2]^{1/2}}$$

and satisfies the condition

$$\left.\frac{\partial v}{\partial \bar{z}}\right|_{\bar{z}=0} = 0 \text{ and } \nabla^2 v = -4\pi\delta(x-\bar{x}, y-\bar{y}, z-\bar{z})$$

Integration of Eq. (A8) is accomplished in the rectangular coordinate system shown in Fig. 10. The coordinate bars and subscripts are now removed with the understanding that scaling factors will be removed and the solution will be finalized in physical coordinates at the end of this development.

Only the solution of the zeroth order boundary value problem will be given to display the method used to obtain the pressures that satisfy the boundary conditions of a swept hingline control surface. All other solutions may be obtained by a similar procedure with the exception of the Poisson equation that needs to be modified before its solution is obtained.

Solution of Zeroth Order Problem

The zeroth order boundary value problem is given as

P. D. E. $\nabla^2 \psi_o = 0$

B. C. $$\frac{\partial \psi_o(x, y, 0)}{\partial z} = -\frac{2\Theta_H}{\beta}\delta(x - y\tan\Lambda)\, U(y) \quad \text{(A9)}$$

Substituting the boundary conditions of Eq. (A9) into Eq. (A8) yields

$$\psi_o(x, y, z) = \frac{\Theta_H}{\pi\beta}\int_0^\infty\int_{-\infty}^\infty \frac{\delta(x' - y'\tan\Lambda_l)\, dx'\, dy'}{[(x-x')^2 + -y-y')^2 + z^2]^{1/2}} \quad \text{(A10)}$$

Performing the indicated integration first in the x' coordinate and then in the y' coordinate and handling the divergent upper limit in the manner of Landahl provides the expression

$$\psi_o(x, y, z) = -\frac{\Theta_H}{\pi\beta}\frac{1}{\sqrt{a}}\log[\sqrt{a}(x^2 + y^2 + z^2)^{1/2} - (y + x\tan\Lambda_l)] + \psi_o(\text{regular}) \quad \text{(A11)}$$

where $a = (1 + \tan^2\Lambda_1)$. Now a check is made to determine whether the boundary conditions are satisfied. The boundary conditions on $z = 0$ plane are evaluated as

$$\frac{\partial \psi_o}{\partial z} = -\frac{\Theta_H}{\pi\beta}\frac{1}{\sqrt{a}} \cdot \left\{\frac{a^{1/2}(x^2 + y^2 + z^2)^{1/2} + (y + x\tan\Lambda_l)}{a(x^2 + y^2 + z^2) - (y^2 + 2xy\tan\Lambda_l + x^2\tan^2\Lambda_l)}\right\} \cdot \frac{\sqrt{a}(z)}{(x^2 + y^2 + z^2)^{1/2}} \quad \text{(A12)}$$

Inserting $a = (1 + \tan^2\Lambda_1)$ into the denominator of the bracketed term and reorganizing results in the expression

$$\frac{\partial \psi_o}{\partial z} = -\frac{\Theta_H}{\pi\beta}\frac{1}{\sqrt{a}}\left\{\sqrt{a} + \frac{(y + x\tan\Lambda_l)}{(x^2 + y^2 + z^2)^{1/2}}\right\} \cdot \frac{\sqrt{a}}{(x - y\tan\Lambda_l)^2 + az^2} \quad \text{(A13)}$$

and noting that

$$\lim_{u \to 0} \frac{u}{x^2 + u^2} = \pi\delta(x)$$

then

$$\left.\frac{\partial \psi_o}{\partial z}\right|_{z \to 0} = -\frac{\Theta_H}{\pi\beta}\frac{1}{\sqrt{a}}\left[\sqrt{a} + \frac{y\sqrt{a}}{|y|}\right]\pi\delta(x - y\tan\Lambda_l)$$

or

$$\left.\frac{\partial \psi_o}{\partial z}\right|_{z \to 0} = -\frac{2\Theta_H}{\beta}\delta(x - y\tan\Lambda_l)\, U(y) \quad \text{(A14)}$$

which is identical to the scaled boundary condition defined in Eq. (A5). Consequently, the function defined by Eq. (A11) is then considered to be a valid solution of the zeroth order boundary value problem.

The expression may be returned to physical coordinates by replacing

$$x \text{ by } \frac{x}{\beta\epsilon};\ y \text{ by } \frac{y}{\epsilon};\ z \text{ by } \frac{z}{\epsilon}$$

$$\tan\Lambda_l \text{ by } \frac{\tan\Lambda}{\beta};\ \sqrt{a} \text{ by } \frac{\bar{\beta}}{\beta};\ \text{and } \bar{\beta}^2 = \beta^2 + \tan^2\Lambda$$

to yield the pressure expression on $z = 0$ plane given as

$$\psi_o(x, y, 0) = -\frac{\Theta_H}{\pi\beta}\log\left[(x^2 + \beta^2 y^2)^{1/2} - \frac{\beta^2 y + x\tan\Lambda}{\bar{\beta}}\right] + \psi_o(\text{regular}) \quad \text{(A15)}$$

The first order boundary value problem (Eq. A6) may be obtained in the manner just described. However, the second order problem needs to be reorganized such that the above method can be applied. The solution is obtained by first seeking a solution of the form

$$\nabla^2 \psi_2^{p\ell} = -\frac{k^2 M^2}{\beta^2}\psi_o \quad \text{(A16a)}$$

$$\left.\frac{\partial \psi_2^{p\ell}}{\partial z}\right|_{z=0} = 0 \quad \text{(A16b)}$$

where

$$\psi_2^{p\ell} = \psi_2^p + \psi_2^\ell$$

That is, a solution is first found for

$$\nabla^2 \psi_2^p = -\frac{k^2 M^2}{\beta^2}\psi_o$$

Next, find the boundary conditions generated by this solution as determined by evaluating

$$\lim_{z\to 0} \frac{\partial \psi_2^g}{\partial z}$$

Then develop a solution ψ_2^ℓ such that

$$\nabla^2 \psi_2^\ell = 0 \tag{A17a}$$

$$\left.\frac{\partial \psi_2^\ell}{\partial z}\right|_{z=0} \equiv -\left.\frac{\partial \psi_2^g}{\partial z}\right|_{z=0} \tag{A17b}$$

then the solution of the Poisson equation is given as

$$\nabla^2 \psi_2^{g\ell} = -\frac{k^2 M^2}{\beta^2}\psi_o \tag{A18a}$$

$$\left.\frac{\partial \psi_2^{g\ell}}{\partial z}\right|_{z=0} \equiv 0 \tag{A18b}$$

One trial function that will suffice for ψ_2^g is

$$\psi_2^g = AR^2 \log(R-\bar{y}) + BR^2$$

where

$$R = (x^2+y^2+z^2)^{1/2}$$
$$\bar{y} = (x\sin\Lambda_l + y\cos\Lambda_l)$$

and the coeffieients A and B are such as to satisfy

$$\nabla^2 \psi_2^g = \left(\frac{k^2M^2}{\beta^2}\cdot\frac{\Theta_H}{\beta}\right)\log[R-\bar{y}] \tag{A19}$$

If the Poisson equation solution is handled in this manner, then the rest of the second-order boundary value problem may be obtained in the manner used on the zeroth-order problem.

The complete solution of the original boundary value problem may now be expressed as a sum of the individual solutions

$$\bar{P}(x,y,0) = (\psi_o + \epsilon\psi_l + \epsilon^2\psi_2)e^{ikM^2x/\beta^2} \tag{A20}$$

or

$$\bar{P}(x,y,0) = C1\cdot\log\left[(x^2+\beta^2y^2)^{1/2} - \left(\frac{\beta^2 y + x\tan\Lambda}{\bar{\beta}}\right)\right]$$
$$+ C2\cdot y\cdot\log[(x^2+\beta^2y^2)^{1/2} - x] \tag{A21}$$

where

$$C1 = -\frac{\Theta_H}{\pi\bar{\beta}}\left\{1+2ik(x-y\tan\Lambda) - \frac{ikM^2\tan\Lambda}{\beta^2\bar{\beta}^2}(x\tan\Lambda + y\beta^2\right.$$
$$-\frac{k^2M^2}{4\beta^2\bar{\beta}^2}(x-y\tan\Lambda)^2 + \frac{k^2M^4\tan^2\Lambda}{4\beta^2\bar{\beta}^4}\left[(x-y\tan\Lambda)^2\right.$$
$$\left.-2\left(\frac{x\tan\Lambda}{\beta}+\beta y\right)^2\right] - \frac{2k^2M^2}{\beta^2}\left[\frac{\beta^2}{2\bar{\beta}^2}(x-y\tan\Lambda)^2\right.$$
$$\left.\left.-(x^2-xy\tan\Lambda)\right] - \frac{k^2}{2}(x-y\tan\Lambda)^2\right\}\cdot e^{ikM^2x/\beta^2}$$

$$C2 = -\frac{\Theta_H}{\pi}\left\{2ik+\left(\frac{2k^2M^2}{\beta^2}-k^2\right)x + \frac{k^2\tan\Lambda}{2}y\right\}\cdot e^{ikM^2x/\beta^2}$$

The expression for $\bar{P}(x,y,0)$ may be simplified by expanding the exponential function, carrying out the indicated multiplication, and collecting terms that are linear in x and y, which yields

$$P(x,y,0) = -\frac{\Theta_H}{\pi\beta}\left[1+2ik(x-x_c) + \frac{ikM^2}{\bar{\beta}^2}(x-x_c)\right]$$
$$\cdot\log\left[(x^2+\beta^2y^2)^{1/2} - \left(\frac{\beta^2y+x\tan\Lambda}{\bar{\beta}}\right)\right]$$
$$-\frac{\Theta_H}{\pi}\left[2ik - k^2(x-x_c) - \frac{k^2}{2}y\tan\Lambda\right]$$
$$\cdot y\cdot\log[(x^2+\beta^2y^2)^{1/2} - x] \tag{A22}$$

For the condition of zero sweep the expression becomes

$$\bar{P}(x,y,0) = -\frac{\Theta_H}{\pi\beta}\left[(1+2ik(x-x_c) + \frac{ikm^2}{\beta^2}(x-x_c)\right]$$
$$\cdot\log\left[(x^2+\beta^2y^2)^{1/2} - \beta y\right] - \frac{\Theta_H}{\pi}\left[2ik - k^2(x-x_c)\right]$$
$$\cdot y\cdot\log\left[(x^2+\beta^2y^2)^{1/2} - x\right] \tag{A23}$$

and is identical to the expression developed by Landahl[5] for the zero sweep control surface case.

Equation (A22) takes on the form of Eq. (8), which was used in the preceding discussion for $k=0$. It should be noted that Eqs. (6), (7), and (8) reduce to the form of Eq. (5), which is Landahl's[5] expression for the case of zero sweep hingelines. However, Eqs. (6) and (7) should be used only for configurations having zero sweep hingelines, or they may be used to approximate the loadings on large span control surface configurations having very small sweep angles by requiring the collocation stations to be located well away from the side edges of the control surface. Equation (A22) may be successfully applied to swept hingeline configurations without the above restrictions.

References

[1] Berman, J. H., Shyprykevich, P., Smedfjeld, J. B., and Kelly, R. F., "Unsteady Aerodynamic Forces in General Wing/Control Surface Configuration in Subsonic Flow," Air Force Flight Dynamics Laboratory, Wright-Patterson AFB, Ohio., AFFDL-TR-67-117 Parts I and II, May 1968.

[2] Rowe, W. S. Winther, B. A., and Redman, M. C., "Unsteady Subsonic Aerodynamic Loadings Caused by Control Surface Motions," *Journal of Aircraft*, Vol. 11, Jan. 1974, pp. 45-54.

[3] Medan, R. T., "Steady, Subsonic, Lifting Surface Theory for Wings With Swept, Partial Span, Trailing Edge Control Surfaces," NASA TND-7251, April 1973.

[4] Hewitt, B. L. "Unsteady Airforces for Wings with Control Surfaces," Agard Symposium Unsteady Aerodynamics for Aeroelastic Analyses of Interfering Surfaces; Ref. No. 14, Part II, AGARD-CP-80-71, Tonsberg, Norway, Nov. 3-4, 1970.

[5] Landahl, M., "Pressure-Loading Functions for Oscillating Wings with Control Surfaces," *AIAA Journal*, Vol. 6, Feb. 1968, pp. 345-348.

[6] Ashley, H. "Subonic Oscillatory or Steady Airloads on Wings With Control Surfaces and Other Discontinuities," Department of Aeronautics and Astronautics, Stanford University, Palo Alto, Calif., No. 336, Dec. 1967.

[7] Darras, B. and Dat, R. "Application de la Theorie de las Surface Portante a des Aiels Munies de Gouvernes," Agard Symposium Unsteady Aerodynamic for Aeroelastic Analyses of Interrering Surfaces; Ref. No. 13, Part II, AGARD-CP-80-71, Tonsberg, Norway , Nov. 3-4, 1970.

[8] Zwaan, R. J., "On a Kernel-Function Method for the Calculation of Pressure Distributions on Wings with Harmonically Oscillating Control Surfaces in Subsonic Flow," NLR TR 70123U, Aug. 3, 1971, (Supersedes, NLR TR 70122U).

[9] Forshcing, H. Treinbstein, H., and Wagener, J., "Pressure Measurements on a Harmonically Oscillating Swept Wing With Two Control Surfaces in Incompressible Flow," Ref. No. 15, Part II, Agard Syposium Unsteady Aerodymamics for Aeroelastic Analyses of Interfering Surfaces; Tonsberg, Norway, Nov. 3-4, 1970. AGARD-CP-80-71.